Journal of Cellular Physiology

Molecular Mechanisms of the Antiproliferative Effect of Beraprost, a Prostacyclin Agonist, in Murine Vascular Smooth Muscle Cells

HENG LIN,[1] JA-LING LEE,[2] HSIN-HAN HOU,[3] CHIH-PENG CHUNG,[4] SUNG-PO HSU,[5] AND SHU-HUI JUAN[2,6,7,8]*

[1]*Institute of Pharmacology and Toxicology, Tzu Chi University, Hualien, Taiwan*

[2]*Graduate Institute of Medical Sciences, Taipei Medical University, Taipei, Taiwan*

[3]*Institute of Biomedical Sciences, Academia Sinica, Taipei, Taiwan*

[4]*Graduate Institute of Cell and Molecular Biology, Taipei Medical University, Taipei, Taiwan*

[5]*Institute of Physiology, College of Medicine, National Taiwan University, Taipei, Taiwan*

[6]*Department of Physiology, Taipei Medical University, Taipei, Taiwan*

[7]*Graduate Institute of Neuroscience, Taipei Medical University, Taipei, Taiwan*

[8]*Topnotch Stroke Research Center, Taipei Medical University, Taipei, Taiwan*

Prostacyclin (PGI_2) has been shown to inhibit proliferation in vascular smooth muscle cells. To clarify the underlying molecular mechanism, we investigated the vasoprotection of beraprost (a PGI_2 agonist) both in vivo and in vitro. Beraprost eliminated increases in proliferation of rat aortic smooth muscle cells (RASMCs) by 12-O-tetradecanoylphorbol 13-acetate, and enhanced the peroxisome proliferator-activated receptor-delta (PPARδ) and inducible nitric oxide synthetase (iNOS) expressions, which were associated with the antiproliferative action of beraprost according to inhibition experiments by [^{3}H]thymidine incorporation. Additionally, elimination of iNOS activity by PPARδ antagonists suggested that iNOS is the downstream target of PPARδ. Furthermore, beraprost increased both consensus PPARδ-responsive element (PPRE)-driven luciferase activity and the binding activity of the PPARδ to the putative PPRE in the iNOS promoter; nevertheless, it was abolished by PPARδ antagonists. Deletion of PPRE (−1,349/−1,330) in the iNOS promoter region (−1,359/+2) strongly reduced promoter-driven activity, representing a novel mechanism of iNOS induction by beraprost. Consistent with this, PPARδ and the concomitant iNOS induction by beraprost were also evident in vivo. Beraprost-mediated protection in a murine model of balloon angioplasty was significantly attenuated by 13S-HODE, a PPARδ antagonist. Taken together, the results suggest that the causal relationship between PPARδ and iNOS contributes to the vasoprotective action of beraprost in RASMCs.

J. Cell. Physiol. 214: 434–441, 2008.

Prostacyclin (PGI_2), produced by vascular endothelium and smooth muscles, has therapeutic effects on the relaxation of smooth muscle and reduction of vascular resistance by direct vasodilation (Hiatt, 2001). Administration of PGI_2 or its stable analogue, iloprost, limits coronary artery disease and infarct size in various animal models (Reynolds et al., 1967; Chiariello et al., 1988). PGI_2 is synthesized by a series of enzymes: cytosolic phospholipase A2 cleaves arachidonic acid (AA) from the sn-2 position of phospholipids, cyclooxygenase (COX) converts AA to PGH_2, and PGI_2 synthetase (PGIS) converts PGH_2 to PGI_2 (Matijevic-Aleksic et al., 1995). Beraprost sodium (BPS), a stable PGI_2 analogue, has been reported to have therapeutic effects on the treatment of primary pulmonary hypertension and obstructive peripheral arterial disease (Lievre et al., 2000; Galie et al., 2002). Similar to the biological properties of PGI_2, BPS can activate adenylate cyclase and increase intracellular cAMP levels through activation of the PGI_2 receptor. On account of its chemical characteristics, BPS is more stable and has higher affinity to the PGI_2 receptor than does natural PGI_2 (Kainoh et al., 1991).

PGI_2 functions through cell surface G protein-coupled receptors linked to different cytoplasmic signaling pathways

Abbreviations: PGI_2, prostacyclin; BPS, beraprost; PPARδ, peroxisome proliferator-activated receptor δ; PPRE, PPARδ-responsive elements; RASMCs, rat aortic smooth muscle cells; TPA, 12-O-tetradecanoylphorbol 13-acetate.

Contract grant sponsor: National Science Council, Taiwan;
Contract grant number: NSC95-2320-B-038-018-MY2.
Contract grant sponsor: Center of Excellence for Clinical Trials and Research in Neurology Specialty.
Contract grant sponsor: Topnotch Stroke Research Center, Ministry of Education.

*Correspondence to: Shu-Hui Juan, Graduate Institute of Medical Sciences and Department of Physiology, Taipei Medical University, 250 Wu-Hsing Street, Taipei 110, Taiwan.
E-mail: juansh@tmu.edu.tw

Received 22 March 2007; Accepted 11 June 2007

DOI: 10.1002/jcp.21214

which exert their effects by interacting with a nuclear hormone receptor, peroxisome proliferator-activated receptor (PPAR) (Vane and Botting, 1995; Prescott and White, 1996). PPARs are members of the nuclear hormone receptor superfamily and are ligand-activated transcription factors. PPARs modulate target gene expression in response to ligand activation after heterodimerization with the retinoid X receptor and binding to peroxisome proliferator-responsive elements (PPREs) of target genes. There are three different PPAR isoforms, designated PPARα, PPARβ (also referred to as PPARδ), and PPARγ, each with distinct physiological functions (Evans et al., 2004; Kim et al., 2005). PPARδ has been shown to be involved in the regulation of lipid metabolism, and potential effects of PPARδ activation are involved in the development of atherosclerotic lesions (Kersten et al., 1999). Moreover, Graham et al. (2005) showed that the potent and selective PPARδ agonist, GW0742X, reduces atherosclerosis in LDLR−/− mice. These observations support an atheroprotective effect of PPARδ agonists in vivo. By contrast, Dressel et al. (2003) showed that PPARδ plays a contrasting role in cardiovascular diseases associated with rat aortic smooth muscle cell (RASMC) proliferation such as atherosclerosis and restenosis. Although there is increased interest in characterizing the roles of PPARδ in numerous disease models, the function of PPARδ remains an enigma.

Numerous studies have focused on the effects of PPARδ on cell viability. For instance, activation of endogenous PPARδ by intracellular PGI_2 produced by expressing PGIS in the human embryonic kidney epithelial 293 cell line promotes apoptosis (Hatae et al., 2001). By contrast, neutralization of PPARδ by sulindac, a nonsteroidal anti-inflammatory drug, suppressed colorectal tumorigenesis in a nude mouse model (He et al., 1999). Therefore, the above-described discrepancies might be due to the effects of PPARδ being tissue and species dependent.

Increasing evidence has shown a close link between PGI_2 and NO. For example, both PGI_2 and NO possess cardioprotective effects in animal models of myocardial infarction. Administration of PGI_2 or its stable analogue, iloprost, or an infusion of authentic NO or NO-donating drugs appears to reduce infarct size in most species studied (Sturzebecher et al., 1989). PGI_2 and NO can interact synergistically and influence each other's synthesis and release. The synergistic antiplatelet activity of PGI_2 and NO in rabbit and human platelets has been demonstrated by a number of workers (Radomski et al., 1987; Macdonald et al., 1988). Haider et al. (2003) demonstrated that COX-2 regulates tumor necrosis factor-mediated G1 shortening, but on the other hand, PGI_2 derived from COX-2 causes nitric oxide-mediated inhibition of vascular smooth muscle cell proliferation. Interestingly, this synergy was not seen in vascular smooth muscles (Lidbury et al., 1989).

In a murine model of carotid artery balloon injury, the activated vascular endothelium produces cytokines and growth factors, which promote the growth and migration of RASMCs, key events in the formation of atherosclerotic lesions in humans. Thus, in addition to the primary culture system, we also examined the role of PPARδ in the proliferation of smooth muscle cells following surgery. Given that PGI_2 and NO influence each other's synthesis and PGI_2 is a ligand of PPARδ, we attempted to delineate the relationship of PPARδ and inducible nitric oxide synthetase (iNOS) induced by PGI_2 and their involvements in the vasoprotective effects of PGI_2 in the vasculature.

Materials and Methods

Isolation and primary culture of RASMCs

RASMCs were isolated from the thoracic aorta of male Sprague–Dawley rats (275–325 g) using the explant technique (Fisher-Dzoga et al., 1973). Briefly, after removal of the endothelium and adventitia, the aortic explants were cultured in DMEM and supplemented with 10% fetal bovine serum, penicillin (100 U/ml), streptomycin (100 μg/ml), and 25 mM HEPES (pH 7.4). After 2 weeks, cells that had migrated out of the explants were removed by trypsinization and successively subcultured. The purity and identity of cells were examined by immunostaining using an antibody specific against smooth muscle cell α-actin. Cells from passages 5 to 12 were used for the experiments.

[^{3}H] Thymidine incorporation

As previously described (Jain et al., 1996), cells at a density of 1×10^4 cells/cm^3 were applied to 24-well plates in DMEM plus 10% fetal bovine serum from Invitrogen (Carlsbad, CA). After the cells had grown to 70–80% confluence, they were rendered quiescent by incubation for 24 h in DMEM containing 2% fetal bovine serum. Chemicals including beraprost (a PGI_2 agonist), 13S-hydroxyoctadecadienoic acid (13S-HODE) (a PPARδ antagonist), and N^G-nitro-L-arginine methyl ester HCL (L-NAME) and N^G-nitro-L-arginine (L-NNA) (NO inhibitors) were purchased from Cayman (Ann Arbor, MI), and 12-O-tetradecanoylphorbol 13-acetate (TPA) (a mitogen), sulindac (a PPARδ antagonist), and sodium nitroprusside dehydrate (SNP) (a NO donor) were purchased form Sigma Chemical (St. Louis, MO). Chemicals as indicated or dimethyl sulfoxide (DMSO) in 10% fetal bovine serum were added to the cells, and the mixture was allowed to incubate for 24 h. During the last 4 h of the incubation with or without beraprost, [^{3}H]thymidine was added at 1 μCi ml^{-1} (1 μCi = 37 kBq). The incorporated [^{3}H]thymidine was extracted in 0.2 N NaOH and measured in a liquid scintillation counter.

MTT assay

The viability of cells was determined based on the activity of mitochondrial dehydrogenase to reduce 3-(4,5-dimethylthiazol-2-yl)-2,5-diphenyl tetrazolium bromide (MTT) (Sigma) to formazan. Briefly, cells were plated in 24-well plates at a density of 1×10^4 cells/well and treated with DMSO or varying concentrations of beraprost for 24 or 48 h. MTT was then added to each well, and incubation continued for 4 h in culture. The formazan formed was dissolved by overnight incubation with 10 mM HCl containing 10% SDS, and then measured at a wavelength of 570 nm.

Electrophoretic mobility shift assay

The electrophoretic mobility shift assay (EMSA) was performed as previously described (Juan et al., 2005). To prepare nuclear protein extracts, cells in 10-cm^2 dishes after treatment with indicated chemicals for 4 h were washed twice with ice-cold PBS and scraped off into 1 ml of PBS. After centrifugation of the cell suspension at 500*g* for 3 min, the supernatant was removed, and cell pellets were subjected to NE-PER™ nuclear extraction reagents (Pierce, Rockford, IL) with the addition of 0.5 mg/ml benzamidine, 2 μg/ml aprotinin, 2 μg/ml leupeptin, and 2 mM PMSF. The subsequence procedures of nuclear protein extraction followed the manufacturer's instructions. The fraction containing the nuclear protein was used for the assay or was stored at −80°C until use. The sequence of the oligonucleotide used was GTGGAGGTCAGGGGACAATT for PPRE binding. The oligonucleotide was end-labeled with [γ-^{32}P]. Extracted nuclear proteins (10 μg) were incubated with 0.1 ng of ^{32}P-labeled DNA for 15 min at room temperature in 25 μl of binding buffer containing 1 μg of poly(deoxyinosine-deoxycytidine) (dI-dC). For competition with unlabeled oligonucleotides, a 100-fold molar excess of unlabeled oligonucleotide relative to the ^{32}P-labeled probe was added to the binding assay. Mixtures were electrophoresed on 5% non-denaturing polyacrylamide gels. Gels were dried and imaged by means of autoradiography.

Transient transfection experiment and luciferase activity assay

Two DNA fragments with or without PPRE of rat iNOS gene promoter sequences from −1,359 to +2 and −1,329 to +2 bp, respectively, were obtained by a polymerase chain reaction (PCR) using rat genomic DNA as the template. The sense and antisense primers were as follows: sense (with PPRE) 5′-TGGTACACATGTGGAGGTCAGGGGACAATT-3′, sense (without PPRE) 5′-TATGGGAGTTTGTTTTCTCCTTCCA-CCGTG-3′, and antisense 5′-CAACTCCCTGTAAAGCTGT-GGCCCTGACAG–3′. The PCR product was flanked with dA and subcloned into the yTA clone vector, which was digested with *Kpn I* and *Sal I* restriction enzymes and subcloned into the *KpnI-XhoI* site of the PGL3-basic vector. The identities of the sequences were confirmed using an ABI PRISM 377 DNA Analysis System (Perkin-Elmer, North Point, Hong Kong).

For the reporter activity assay, cells were seeded in six-well plates at a density of 1×10^5 cells/well. In brief, RASMCs were transiently transfected with 1.05 μg of plasmid DNA containing 0.05 μg of the Renilla luciferase construct, pRL-TK (Promega, Madison, WI), to control transfection efficiency and 1 μg of the appropriate iNOS promoter firefly luciferase (FL) construct. The next day, cells were transfected with pGL3/iNOS promoter variants (−1,359/+2 or −1,329/+2) and pRL-TK (the internal control plasmid) using LipofectAMINE 2000™ (Invitrogen). After transfection for 4 h, the medium was replaced with complete medium, and incubation continued for another 20 h. Transfected cells were then treated with drugs for 12 h, and cell lysates were collected. Luciferase activities were recorded in a TD-20/20 luminometer (Turner Designs, Sunnyvale, CA) using the dual luciferase assay kit (Promega) according to the manufacturer's instructions. Luciferase activities of the reported plasmids were normalized to luciferase activities of the internal control plasmid.

RNA Isolation and analysis of gene expression by real-time-PCR

Total RNA was prepared from cultures by directly lysing cells in Trizol buffer (Life Technologies, Gaithersburg, MD), and mRNAs were reversed-transcribed into cDNA using oligo-dT and reverse transcriptase (Invitrogen). After first-strand cDNA synthesis, it was used as a template and amplified by pairs of primers derived from PPARδ and iNOS genes for RT-PCR and quantitative real-time-polymerase chain reaction (RT-PCR) analysis. Sequences of the primer pairs for amplification of each gene were 5′-AACATCCCCAACTTCAGCAG-3′ and 5′-TACTGCGCAAGAACTCATGG-3′ (for the PPARδ gene); 5′-ACCTGAAAGAGGAAAAGGAC-3′ and 5-CTCTGGTC-AAACTCTTGGAG–3′ (for the iNOS gene); and 5′-CCACCATGGAGAAGGCTGGGGCTCA-3′ and 5′-ATCACGCCACAGTTTCCCGGAGGGG-3′ (for the GAPDHgene). PCR amplifications were conducted using QPCRMaster Mixture and SYBER Green-based detection™ systems (ABI; Applied Biosystems, Foster City, CA) according to the manufacturer's instructions, with 100 nM primers and 100 ng of cDNA template in a 20-μl reaction volume. Thermocycling was initiated by 2 min of decontamination at 50°C and 10 min of hot start at 95°C, followed by 40 cycles of 95°C for 15 sec, 55°C for 30 sec, and 60°C for 60 sec, with a single fluorescence reading taken at the end of each cycle. Each run was completed with a melting curve analysis to confirm the specificity of amplification and lack of primer dimers. Ct values were determined by the ABI System Software using a fluorescence threshold manually set to 0.0160. Individual gene expression Ct values at various time points were normalized by subtracting the respective Ct value of a housekeeping gene, GAPDH, to obtain a ΔCt calibrated value. Experimental samples are presented as multiples of induction with respect to each control group at various time points.

Western blots

Western blotting was carried out with a rabbit polyclonal anti-PPARδ antibody, rabbit polyclonal anti-iNOS antibody (Santa Cruz; Santa Cruz, CA), and mouse polyclonal anti-GAPDH antibody (Biogenesis; Kingston, NH). Cell lysate (50 μg) was electrophoresed on an 8% SDS–polyacrylamide gel and then transblotted onto a Hybond-P membrane (GE Healthcare, Mongkok, Hong Kong). The blot was blocked in PBS containing 0.1% Tween-20 and 5% skim milk at room temperature for 1 h, followed by incubation with the first antibody (diluted 1: 1,000) for another hour in PBS containing 0.1% Tween-20 and 5% skim milk. After 2 washes, the blot was incubated with peroxidase-conjugated goat anti-rabbit immunoglobulin G (IgG)/anti-mouse IgG (1: 2,000) (Sigma) (diluted 1: 2,000) for an additional 1 h. Antigen was detected with an enhanced chemiluminescence system (GE Healthcare).

Nitrite assay

RASMCs were plated at a density of 1×10^5 cells/ml in 24-well plates for 16 h, followed by treatment with beraprost (1 μM) or the addition of various concentrations of PPARδ antagonists for a further 24 h. The amount of NO production in the medium was detected with the Griess reaction. One hundred microliters of each supernatant was mixed with the same volume of Griess reagent (1% sulfanilamide in 5% phosphoric acid and 0.1% naphthylethylenediamine dihydrochloride in water). The absorbance of the mixture at 530 nm was determined with an enzyme-linked immunosorbent assay (ELISA) plate reader (Dynatech MR-7000; Dynatech Laboratories).

Carotid injury

Animal care and treatment were conducted in conformity with the protocols of the Animal Center, Taipei Medical University. Male C57B6 mice (6–10 weeks old, 25.8 ± 1.8 g) were used in this study. Animals were anesthetized intramuscularly with a combination of ketamine (8 mg/100 g body weight), xylazine (2 mg/100 g), and atropine (0.16 mg/100 g). The right carotid artery was exposed, and endothelial denudation of the common carotid was induced with a 29-gauge needle (0.35 mm in diameter), the tip of which was roughened and coated with an α-cyanoacrylate bead (0.5 mm in diameter). This modified needle was then introduced through the internal carotid artery and moved into the common carotid artery. The common carotid artery was abraded four times. The arteriotomy site was ligated, and the skin was closed using sutures. The external carotid was then tied off, and blood flow was restored through the common carotid artery. The mice recovered from anesthesia and were allowed free access to food and water. Nalbuphine (1–2 mg/kg intramuscularly) was given as the postoperative analgesia. After carotid balloon injury, mice were divided into four groups: saline as the control, beraprost alone, PPARδ antagonist (13S-HODE), and beraprost combined with 13S-HODE (with six mice in each group). Balloon-injured mice were subcutaneously given beraprost (1 mg/kg) on day 2 or 13S-HODE (100 μg/kg) on day 3 following surgery, and separate chemicals were given every other day for 2 weeks. Furthermore, mice without balloon injury were given saline, beraprost, or 13S-HODE as the controls.

Histological analysis and quantification of atherosclerotic lesions

Animals were killed 2 weeks after vascular injury. The operated carotid arteries were excised, fixed in 4% paraformaldehyde, embedded in paraffin, and serially sectioned at 7 μm for histological staining or other experiments. Totally, 100 sections from each injured artery were collected. In total, 11 sections sampled from every 10 consecutive sections were stained with Verhoeff van Gieson elastic stain and used for lesion estimation (Lee et al., 1999).

Immunohistochemistry

Immunostaining was carried out using the same antibodies as in the Western blot analysis. Tissue sections were pretreated with 3% H_2O_2 for 15 min at room temperature. After incubation in PBS containing 2% bovine serum albumin (BSA) at 37°C for 30 min, sections were incubated with the primary antibody at 37°C for 30 min, followed by three washes in PBS. Sections were then incubated with a horseradish peroxidase-conjugated secondary antibody for another 30 min. After three washes, color was developed with 0.1% 3,3′-diaminobenzidine/0.01% H_2O_2. Pictures were taken at a 200× magnification using a CCD camera (DP70, Olympus, Melville, NY) attached to a microscope system (BX51, Olympus).

Statistical analysis

Values are expressed as the mean ± SD The significance of the difference from the control groups was analyzed by Student's *t*-test or one-way analysis of variance (ANOVA) and Bonferroni's method as a post hoc test. A value of $P < 0.05$ was considered statistically significant.

Results

Effects of beraprost on cell proliferation and cell viability

To examine the specificity of a direct effect of PGI_2 on cellular proliferation, we performed [^{3}H]thymidine incorporation in RASMCs in the presence of various concentrations of beraprost, a PGI_2 agonist. Beraprost not only concentration-dependently inhibited [^{3}H]thymidine incorporation into RASMCs by about 36%, but also reversed TPA-induced DNA synthesis by about 50%, as shown in Figure 1A. In addition, to examine the effect of cell viability by beraprost, an MTT assay was carried out. Beraprost concentration-dependently inhibited cell viability on day 2 by approximately 30%, but not on day 1, as illustrated in Figure 1B.

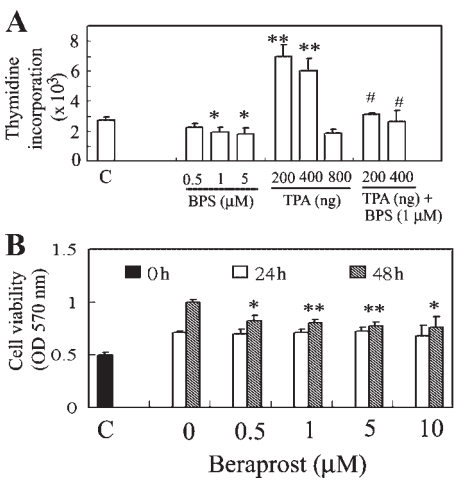

Fig. 1. Effects of beraprost (BPS) on DNA synthesis and viability of rat aortic smooth muscle cells (RASMCs). A: BPS concentration-dependently inhibited DNA synthesis and reversed the 12-O-tetradecanoylphorbol 13-acetate (TPA)-induced cell proliferation by [^{3}H]thymidine incorporation in RASMCs. Cells were pretreated with TPA for 1 h prior to additional BPS treatment. Data are shown as the mean ± SD of five independent experiments. $^*P < 0.05$ and $^{**}P < 0.01$ versus the control group; $^{\#}P < 0.01$ versus TPA treatment alone. B: BPS decreased cell viability at 2 days after treatment. The cell viability of cells in 24-well plates treated with BPS was determined by the MTT assay at the indicated time points. Data shown are the mean ± SD of five independent experiments. Significantly different ($^*P < 0.05$ and $^{**}P < 0.01$ versus the DMSO-treated group at day 2).

Time-dependent inductions of PPARδ and iNOS, and an increase in NO production by beraprost

To unravel the close linkages among PGI_2, NO, and PPARδ, we analyzed the time-dependent inductions of PPARδ and iNOS by beraprost in RASMCs at both the mRNA and protein levels. RNA and total cell lysate were harvested from RASMCs treated with 1 μM beraprost for 2, 4, 6, 12, or 24 h, as analyzed by real-time-PCR, RT-PCR, and Western blotting. As illustrated in Figure 2A,B, beraprost significantly increased induction of PPARδ at as early as 2 h, whereas induction of iNOS was observed at 4 h after treatment. Time-course inductions of PPARδ and iNOS by BPS from 0 to 12 h increased by approximately 1.5-fold to 3.6-fold and 1.2-fold to 2.9-fold, respectively. Additionally, the nitrite assay in Figure 2C demonstrated that beraprost significantly stimulated NO production no earlier than 4 h after treatment; this time point is consistent with the findings in Figure 2A,B, regarding iNOS induction by beraprost at both the RNA and protein levels. NO production was increased approximately twofold at 24 h after 1 μM BPS treatment in RASMCs.

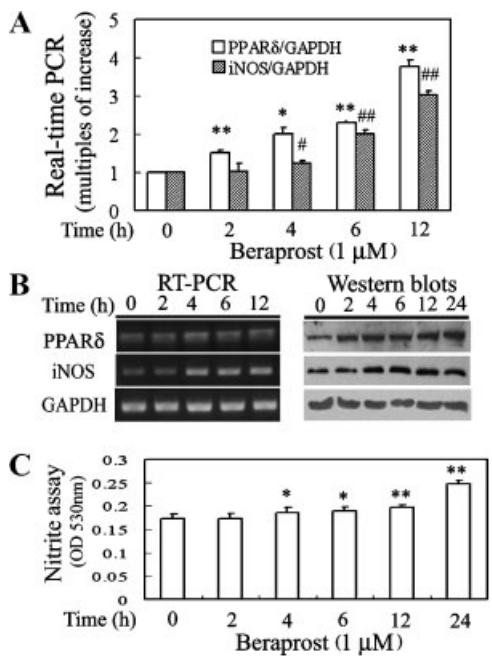

Fig. 2. Induction of PPARδ and iNOS by beraprost in RASMCs. A: Time-course induction of PPARδ and iNOS by beraprost. Total RNA was extracted and analyzed by real-time-PCR; the methods are described in Section "Materials and Methods." Cells were treated with beraprost (1 μM) for 2, 4, 6, 12, or 24 h. Four samples were analyzed in each group, and values are presented as the mean ± SD. Significantly different ($^*P < 0.05$ and $^{**}P < 0.01$ vs. PPARδ/GAPDH at hour 0, $^{\#}P < 0.05$ and $^{\#\#}P < 0.01$ vs. iNOS/GAPDH at hour 0). B: Induction of both mRNA and protein levels of PPARδ and iNOS by beraprost. Equal loading in each lane or transfer was confirmed using GAPDH mRNA or by incubating with an anti-GAPDH antibody. Representative results of three separate experiments are shown. C: Increase in NO release by beraprost. NO production in the medium by beraprost was measured by the Griess reaction. Six samples were analyzed in each group, and values are presented as the mean ± SD. Significantly different ($^*P < 0.05$, $^{**}P < 0.01$).

Decrease in iNOS expression and NO production by PPARδ antagonists

Results in Figure 2 show that the time frame of PPARδ induction was approximately 2 h earlier than that of iNOS by beraprost. In order to examine the causal relationship between PPARδ and iNOS, we used the PPARδ antagonists, 13S-HODE and sulindac, to investigate their effects on iNOS expression. A nitrite assay analysis (Fig. 3A) demonstrated that PPARδ antagonists statistically inhibited beraprost-induced NO production in an amount similar to the control group after 24 h of treatment, suggesting that iNOS is the downstream target of PPARδ. Moreover, cells pretreated with PPARδ antagonists (sulindac or 13S-HODE) for 1 h prior to the addition of beraprost, showed decreased protein levels of iNOS as a result of a decrease in PPARδ protein expression, as shown in Figure 3B by Western blotting.

Transcriptional regulation of iNOS by PPARδ in RASMCs treated with beraprost

As it is known that PGI_2 exerts its function through PPARδ and has a close link with nitric-oxide synthetase (NOS) (Sturzebecher et al., 1989; Vane and Botting, 1995; Narumiya et al., 1999), we also demonstrated in Figure 2 that beraprost induced both PPARδ and iNOS expression; the time frame of PPARδ's action was earlier than that of iNOS. Therefore, we constructed two repeats of the consensus PPARδ-responsive element (PPRE) in the pGL2-promoter vector. Beraprost concentration-dependently enhanced the luciferase activity by approximately 1.6-fold to 5.6-fold in cells transfected with the PPRE construct as shown in Figure 4A. The putative PPRE in the iNOS promoter region as analyzed by the MOTIF Search software was synthesized and used as a probe for an EMSA. The results presented in Figure 4B show that beraprost increased the DNA binding activity of PPARδ to the putative PPRE, whereas the activity was alleviated by PPARδ antagonists.

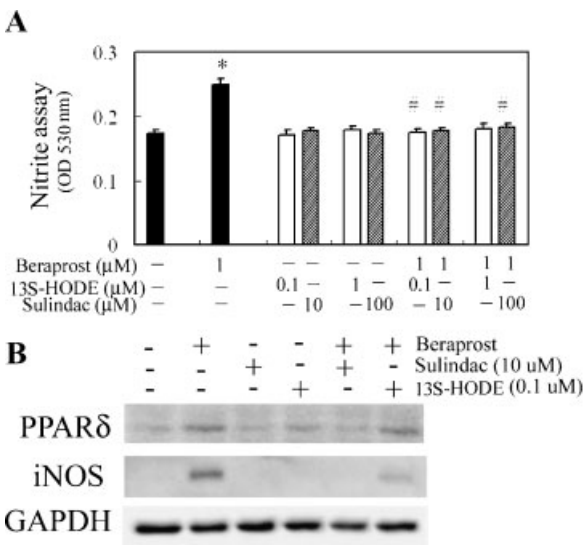

Fig. 3. Effects of the PPARδ antagonists, sulindac (10 and 100 μM) and 13S-HODE (0.1 and 1 μM), on NO production in RASMC exposed to beraprost (A) and protein levels of PPARδ and iNOS by Western blots (B). Six samples were analyzed in each group, and values are presented as the mean ± SD. Significantly different (*$P < 0.05$ vs. the DMSO-treated group, #$P < 0.05$ vs. BPS alone). GAPDH was used as an internal control, and results shown were reproduced in three separate experiments.

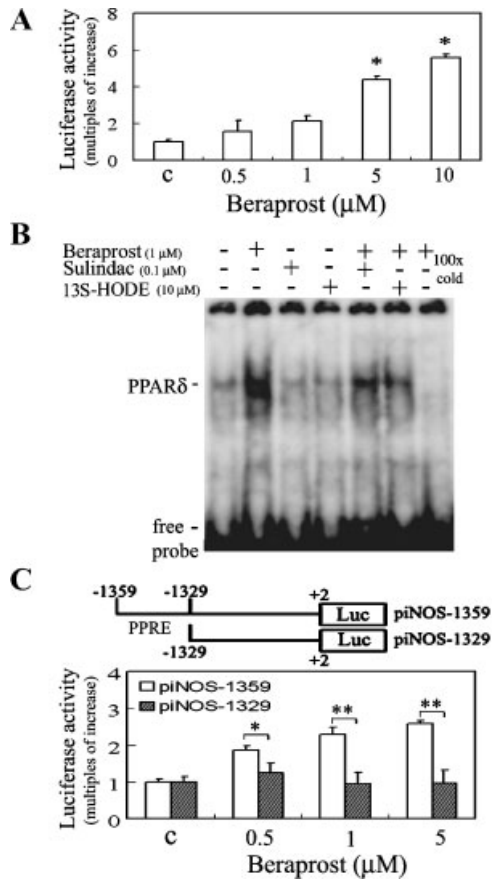

Fig. 4. Binding activity of PPARδ to the PPRE in relation to beraprost or its antagonists. A: A concentration-dependent increase in consensus PPRE-driven luciferase activity by beraprost. Luciferase activities of the reported plasmid were normalized to those of the internal control and are presented as the mean ± SD. Significantly different (*$P < 0.05$ vs. the DMSO-treated group, #$P < 0.05$ and ##$P < 0.01$ vs. the piNOS-1,329 group). B: A decrease in the binding activity of PPARδ to the PPRE by PPARδ antagonists. Cells were cultured and pretreated with PPARδ antagonists for 1 h prior to the addition of 1 μM beraprost. The putative PPRE binding activity derived from the iNOS promoter region of nuclear proteins was assayed by EMSA. 100× cold denotes a 100-fold molar excess of unlabeled oligonucleotides relative to the ^{32}P-labeled probe; this was added to the binding assay for competition with the unlabeled oligonucleotide. The mobility of specific PPRE complexes is indicated. Representative results of three separate experiments are shown. C: Importance of the putative PPREδ in iNOS promoter-driven luciferase activity by beraprost. Luciferase constructs of iNOS promoter variants were obtained as described in Section "Materials and Methods." The experimental reporter luciferase activity was calculated by subtracting the intrinsic activity as measured by samples corresponding to the pGL3-basic vector and then normalizing them to the transfection efficiencies as measured by the activity derived from pRL-TK. Data are presented as the mean ± SD. Significantly different (*$P < 0.05$ vs. the DMSO-treated group or *$P < 0.05$ and **$P < 0.01$ vs. the piNOS-1,359 group treated with the indicated concentrations of beraprost).

Another approach, consisting of luciferase constructs of the rat iNOS promoter regions (−1,359/+2) with or without the putative PPRE (−1,349/−1,330) by deletion mutation, was used to confirm that the binding of PPARδ to the PPRE is associated with transactivation of iNOS by beraprost. The wild-type construct was transiently transfected into RASMCs for 24 h followed by the addition of the indicated concentrations of beraprost. After incubation for another 12 h, cells were

harvested and analyzed for luciferase activity. As shown in Figure 4C, luciferase activity increased by about twofold to 2.6-fold in response to increased concentrations of beraprost of from 0.5 to 5 μM. In contrast, the concentration-dependent increase in promoter activity by beraprost was abolished when the putative PPRE was removed, as shown in Figure 4C.

Reversal of beraprost-induced inhibition of RASMCs DNA synthesis by PPARδ and NO inhibitors, and a mimicking of the effect of beraprost by sodium nitroprusside dehydrate (SNP), a NO donor

To examine whether PPARδ and iNOS are responsible for the antiproliferative effects of beraprost in RASMCs, their individual antagonists or inhibitors were utilized to investigate this postulation. We show in Figure 5A,B, that the PPARδ antagonist and NO inhibitors significantly reversed the decrease in DNA synthesis by beraprost in the [^{3}H]thymidine incorporation assay, suggesting that beraprost's actions are exerted through PPARδ and NO. Conversely, SNP, a NO donor, was used to mimic this effect of beraprost in RASMCs. As shown in Figure 5C, SNP at concentrations of 0.1–10 μM, similar to those of beraprost, caused a statistically significant decrease in DNA synthesis in the [^{3}H]thymidine incorporation experiment.

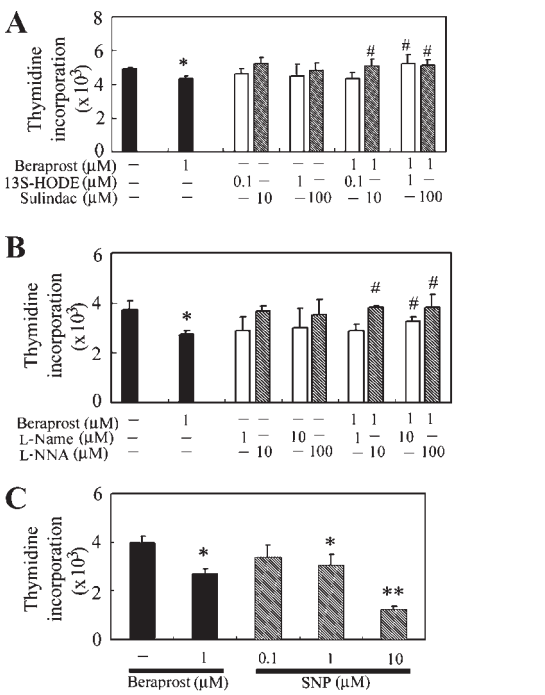

Fig. 5. Abolishment of beraprost-induced decrease in cell proliferation by the PPARδ antagonists, sulindac and 13S-HODE (A), and by the NO inhibitors, L-NNA and L-NAME (B), and sodium nitroprusside dehydrate (SNP), a NO donor, mimicking the effect of beraprost in RASMCs (C). The effects of PPARδ antagonists or iNOS inhibitors on berapost-induced DNA synthesis inhibition, or SNP mimicking the effects of BPS were assessed by [^{3}H]thymidine incorporation, as described in Section "Materials and Methods." RASMCs were pretreated with PGI_2 antagonists or NO inhibitors for 1 h prior to the addition of 1 μM beraprost, or cells were treated with increasing concentrations of SNP and then incubation continued for another 24 h. Six samples were analyzed in each group, and values represent the mean ± SD. Significantly different ($^*P < 0.05$ and $^{**}P < 0.01$ vs. the DMSO-treated group, $^{\#}P < 0.05$ vs. BPS alone).

Therapeutic effects and mechanisms of beraprost in mice subjected to carotid balloon injury

An animal model of carotid balloon injury was established to examine the antiproliferative effects of beraprost in vivo. Carotid balloon injury is the commonest procedure to simulate the pathology of atherosclerosis; the key feature is smooth muscle cell overproliferation. We demonstrate in Figure 6A,B that balloon-injured mice given beraprost as therapeutic treatment showed decreased progression of restenosis by about 70% compared to injured mice alone. Additionally, 13S-HODE, a PPARδ antagonist, was used to examine whether PPARδ is the key player exerting the antiproliferation effects of beraprost in RASMCs. Indeed, the addition of the PPARδ antagonist blocked the antiproliferative effect of beraprost, resulting in increased progression of restenosis compared with

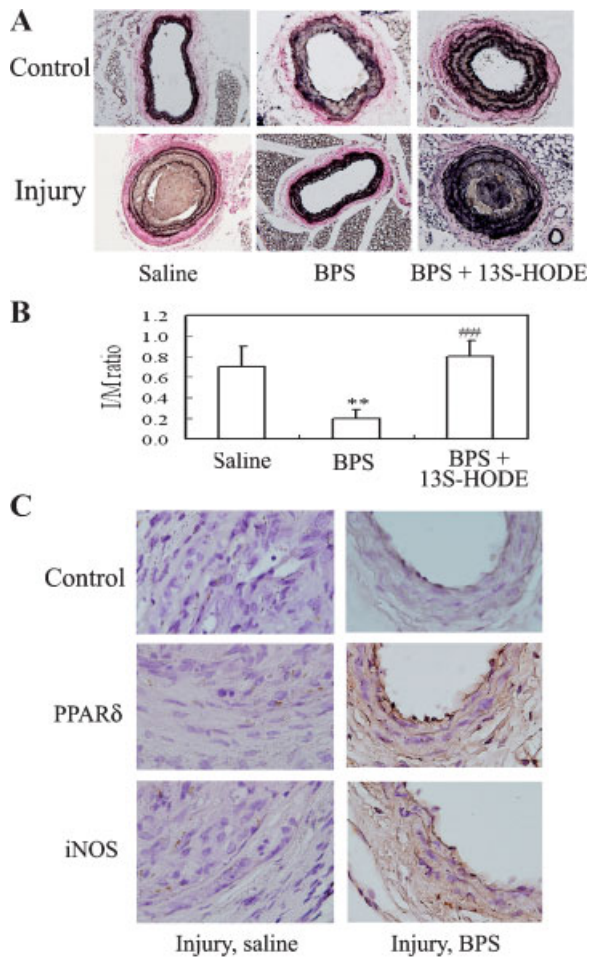

Fig. 6. Effect of beraprost (BPS) or in combination with 13S-HODE on neointimal formation. The carotid arteries of mice were subjected to angioplasty and subsequent treatment with saline, BPS alone, or BPS in combination with 13S-HODE. At 2 weeks after injury, neointimal formation was examined. A: Verhoeff van Gieson staining of injured arterial segments. B: Intima/media (I/M) ratios of injured arteries in various treated groups. The thicknesses of the intima and media of injured arteries were quantified as described in Section "Materials and Methods." The number of animals in each group was six. $^{**}P < 0.01$ versus the saline group and $^{\#\#}P < 0.01$ versus the BPS-treated group. C: The extents of BPS-induced PPARδ and iNOS expressions were examined by immunostaining with the indicated antibodies. [Color figure can be viewed in the online issue, which is available at www.interscience.wiley.com.]

the experimental group treated with beraprost alone, which suggests the important role of PPARδ in the antiproliferative action of beraprost in balloon injury. Furthermore, histoimmunochemical staining showed that beraprost treatment caused the induction of PPARδ and iNOS (Fig. 6C) which agrees with the in vitro findings.

Discussion

In this study, we provide both in vitro and in vivo data to support the roles of PPARδ and iNOS in the antiproliferative action of beraprost, a PGI_2 agonist, in RASMCs. Antagonists or inhibitors of PPARδ and iNOS were utilized to reverse a decrease in DNA synthesis of RASMCs by beraprost. We also clearly delineate the causal relationship between PPARδ and iNOS, as PPARδ antagonists decreased the protein levels of iNOS and NO production. Furthermore, a deletion mutation identified a functional PPRE located in the promoter region of the murine iNOS gene by the promoter luciferase assay, suggesting that PPARδ is an upstream effecter of iNOS induction by beraprost.

In the present study, we examined the potential effects of PPARδ induced by beraprost on the inhibition of vascular smooth muscle proliferation and its implications in the prevention of restenosis after carotid balloon injury in vivo. Apparently, the present finding is contradictory to a recent report showing that PPARδ induced by PDGF or by carotid balloon injury promoted cell proliferation in RASMCs (Zhang et al., 2002). The discrepancy of PPARδ on RASMC proliferation might be attributed to whether it is properly ligand-bonded (i.e., beraprost, a PGI_2 agonist, a natural ligand of PPARδ) or what its inducers are, although this speculation remains to be further investigated. Nevertheless, a very recent study by Graham et al. (2005) with outcomes similar to our findings demonstrated the atheroprotective effect of the PPARδ agonist, GW0742, in $LDLR^{-/-}$ mice by showing a decrease in the chemotactic and proinflammatory molecules (Graham et al., 2005).

It has been documented that an intracellular or extracellular source of PGI_2 produces different cell fates. For instance, Hatae et al. (2001) demonstrated that intracellular PGI_2 formed by expressing PGIS in human embryonic kidney 293 cells promotes apoptosis by activating PPARδ. Conversely, iloprost (an extracellular PGI_2) or dibutyryl cAMP (a cAMP agonist) reduced apoptosis. Furthermore, Ii et al. (2001) demonstrated that beraprost, an extracellular PGI_2 source, reduces RASMCs proliferation through cAMP signaling by preventing downregulation of p27. In our study, we provide another line of evidence showing that even though beraprost is an extracellular PGI_2 source, it can activate PPARδ with a concomitant induction of iNOS to exert the antiproliferative action of PGI_2 in RASMCs. Likewise, the antiproliferative effect of beraprost in RASMCs was limited to cell cycle arrest, as no apoptotic cell death was observed (data not shown) in our study, similar to the findings of Ii et al. (2001).

Additionally, a deletion mutation of the putative PPRE revealed that a functional PPRE in the promoter region of iNOS is associated with the induction of iNOS by the luciferase promoter assay (Fig. 4C). This causal relationship between PPAR and NO is in accord with a recent study by Crosby et al. (2005) showing that a novel PPARγ-responsive element in the promoter region of iNOS has been identified in rat mensangial cells, which contributes positive basal expression and negative expression of iNOS in response to inflammatory stimuli. Likewise, Niwano et al. (2003) demonstrated that beraprost transcriptionally stimulates eNOS expression in vascular endothelial cells, although it is transcriptionally activated by a cAMP-responsive element. The synergistic activity of PGI_2 and NO has been manifested in various tissues (Radomski et al., 1987; Macdonald et al., 1988), but not in vascular smooth muscle cells (Lidbury et al., 1989); nevertheless, we demonstrate that their causal relationship is involved in the antiproliferation of RASMCs. In view of the still not clearly determined role of PPARδ in the physical and pathological remodeling of the vasculature, we demonstrate a correlation of PPARδ with iNOS induction by PGI_2 to exert its antiproliferative effect in RASMCs both in vivo and in vitro.

In summary, the data presented herein provide evidence to support the essential role of PPARδ in the antiproliferative function of beraprost, although the cellular signal pathway by which beraprost induces PPARδ expression remains to be determined. PPARδ appears to transcriptionally mediate the upregulation of iNOS in RASMCs. Identifying the proteins including PPARδ and iNOS responsible for the antiproliferation of RASMCs by beraprost will provide an important molecular basis for the design of new therapeutic strategies to treat atherosclerosis, restenosis or stroke.

Literature Cited

Chiariello M, Golino P, Cappelli-Bigazzi M, Ambrosio G, Tritto I, Salvatore M. 1988. Reduction in infarct size by the prostacyclin analogue iloprost (ZK 36374) after experimental coronary artery occlusion-reperfusion. Am Heart J 115:499–504.

Crosby MB, Svenson J, Gilkeson GS, Nowling TK. 2005. A novel PPAR response element in the murine iNOS promoter. Mol Immunol 42:1303–1310.

Dressel U, Allen TL, Pippal JB, Rohde PR, Lau P, Muscat GE. 2003. The peroxisome proliferator-activated receptor beta/delta agonist, GW501516, regulates the expression of genes involved in lipid catabolism and energy uncoupling in skeletal muscle cells. Mol Endocrinol (Baltimore, MD) 17:2477–2493.

Evans RM, Barish GD, Wang YX. 2004. PPARs and the complex journey to obesity. Nat Med 10:355–361.

Fisher-Dzoga K, Jones RM, Vesselinovitch D, Wissler RW. 1973. Ultrastructural and immunohistochemical studies of primary cultures of aortic medial cells. Exp Mol Pathol 18:162–176.

Galie N, Humbert M, Vachiery JL, Vizza CD, Kneussl M, Manes A, Sitbon O, Torbicki A, Delcroix M, Naeije R, Hoeper M, Chaouat A, Morand S, Besse B, Simonneau G. 2002. Effects of beraprost sodium, an oral prostacyclin analogue, in patients with pulmonary arterial hypertension: A randomized, double-blind, placebo-controlled trial. J Am Coll Cardiol 39:1496–1502.

Graham TL, Mookherjee C, Suckling KE, Palmer CN, Patel L. 2005. The PPARdelta agonist GW0742X reduces atherosclerosis in LDLR(−/−) mice. Atherosclerosis 181:29–37.

Haider A, Lee I, Grabarek J, Darzynkiewicz Z, Ferreri NR. 2003. Dual functionality of cyclooxygenase-2 as a regulator of tumor necrosis factor-mediated G1 shortening and nitric oxide-mediated inhibition of vascular smooth muscle cell proliferation. Circulation 108:1015–1021.

Hatae T, Wada M, Yokoyama C, Shimonishi M, Tanabe T. 2001. Prostacyclin-dependent apoptosis mediated by PPAR delta. J Biol Chem 276:46260–46267.

He TC, Chan TA, Vogelstein B, Kinzler KW. 1999. PPARdelta is an APC-regulated target of nonsteroidal anti-inflammatory drugs. Cell 99:335–345.

Hiatt WR. 2001. Medical treatment of peripheral arterial disease and claudication. New Engl J Med 344:1608–1621.

Ii M, Hoshiga M, Fukui R, Negoro N, Nakakoji T, Nishiguchi F, Kohbayashi E, Ishihara T, Hanafusa T. 2001. Beraprost sodium regulates cell cycle in vascular smooth muscle cells through cAMP signaling by preventing down-regulation of p27(Kip1). Cardiovasc Res 52:500–508.

Jain M, He Q, Lee WS, Kashiki S, Foster LC, Tsai JC, Lee ME, Haber E. 1996. Role of CD44 in the reaction of vascular smooth muscle cells to arterial wall injury. J Clin Invest 97:596–603.

Juan SH, Cheng TH, Lin HC, Chu YL, Lee WS. 2005. Mechanism of concentration-dependent induction of heme oxygenase-1 by resveratrol in human aortic smooth muscle cells. Biochem Pharmacol 69:41–48.

Kainoh M, Maruyama I, Nishio S, Nakadate T. 1991. Enhancement by beraprost sodium, a stable analogue of prostacyclin, in thrombomodulin expression on membrane surface of cultured vascular endothelial cells via increase in cyclic AMP level. Biochem Pharmacol 41:1135–1140.

Kersten S, Seydoux J, Peters JM, Gonzalez FJ, Desvergne B, Wahli W. 1999. Peroxisome proliferator-activated receptor alpha mediates the adaptive response to fasting. J Clin Invest 103:1489–1498.

Kim DJ, Murray IA, Burns AM, Gonzalez FJ, Perdew GH, Peters JM. 2005. Peroxisome proliferator-activated receptor-beta/delta inhibits epidermal cell proliferation by down-regulation of kinase activity. J Biol Chem 280:9519–9527.

Lee TS, Shiao MS, Pan CC, Chau LY. 1999. Iron-deficient diet reduces atherosclerotic lesions in apoE-deficient mice. Circulation 99:1222–1229.

Lidbury PS, Antunes E, de Nucci G, Vane JR. 1989. Interactions of iloprost and sodium nitroprusside on vascular smooth muscle and platelet aggregation. Br J Pharmacol 98:1275–1280.

Lievre M, Morand S, Besse B, Fiessinger JN, Boissel JP. 2000. Oral beraprost sodium, a prostaglandin I(2) analogue, for intermittent claudication: A double-blind, randomized, multicenter controlled trial. Beraprost et Claudication Intermittente (BERCI) Research Group. Circulation 102:426–431.

Macdonald PS, Read MA, Dusting GJ. 1988. Synergistic inhibition of platelet aggregation by endothelium-derived relaxing factor and prostacyclin. Thromb Res 49:437–449.

Matijevic-Aleksic N, Sanduja SK, Wang LH, Wu KK. 1995. Differential expression of thromboxane A synthetase and prostaglandin H synthetase in megakaryocytic cell line. Biochim Biophys Acta 1269:167–175.

Narumiya S, Sugimoto Y, Ushikubi F. 1999. Prostanoid receptors: Structures, properties, and functions. Physiol Rev 79:1193–1226.
Niwano K, Arai M, Tomaru K, Uchiyama T, Ohyama Y, Kurabayashi M. 2003. Transcriptional stimulation of the eNOS gene by the stable prostacyclin analogue beraprost is mediated through cAMP-responsive element in vascular endothelial cells: Close link between PGI2 signal and NO pathways. Circ Res 93:523–530.
Prescott SM, White RL. 1996. Self-promotion? Intimate connections between APC and prostaglandin H synthetase-2. Cell 87:783–786.
Radomski MW, Palmer RM, Moncada S. 1987. The anti-aggregating properties of vascular endothelium: Interactions between prostacyclin and nitric oxide. Br J Pharmacol 92:639–646.
Reynolds EW, Jr., Muller BF, Anderson GJ, Muller BT. 1967. High-frequency components in the electrocardiogram. A comparative study of normals and patients with myocardial disease. Circulation 35:195–206.
Sturzebecher S, McDonald FM, Grundmann G, Hartmann S, Lammert C. 1989. Myocardial ischaemia and reperfusion in the anaesthetised pig: Reduction of infarct size and myocardial enzyme release by the stable prostacyclin analogue iloprost. Prog Clin Biol Res 301:155–159.
Vane JR, Botting RM. 1995. Pharmacodynamic profile of prostacyclin. Am J Cardiol 75:3A–10A.
Zhang J, Fu M, Zhu X, Xiao Y, Mou Y, Zheng H, Akinbami MA, Wang Q, Chen YE. 2002. Peroxisome proliferator-activated receptor delta is up-regulated during vascular lesion formation and promotes post-confluent cell proliferation in vascular smooth muscle cells. J Biol Chem 277:11505–11512.